Electrocatalysis (2017) 8:647–656
DOI 10.1007/s12678-017-0403-9

ORIGINAL ARTICLE

Theoretical Studies on the CO_2 Reduction to CH_3OH on Cu(211)

Shan Ping Liu[1] · **Ming Zhao**[1] · **Wang Gao**[1] · **Qing Jiang**[1] · **Timo Jacob**[2]

Published online: 1 August 2017

Abstract CO_2 reduction has been pursued for decades as an effective way to produce useful fuels and to mitigate global warming at the same time. Methanol synthesis from CO_2 hydrogenation over Cu-based catalysts plays an important role in the chemical and energy industries. However, fundamental questions regarding the reaction mechanism and key reaction intermediates of this process are still unclear. To address these issues, we studied the CO_2 hydrogenation process using density functional theory (DFT) combined with van der Waals (vdW) force corrections, finding that the most effective pathway proceeds along the reaction series CO* → CHO* → CH_2O* → CH_2OH* → CH_3OH* with the reactive intermediate CH_2O*, which is consistent with experimental findings. Additionally, we find that water molecules play an inhibiting role in the reaction, while H bonds and vdW forces have an essential effect on the reaction mechanisms. These findings shed light on the reaction mechanism of CH_3OH formation from CO_2 hydrogenation and reveal the essence of H_2O in this reaction, providing a useful basis for preceding studies.

Keywords Density functional theory · CO_2 reduction · Electrocatalysis · Copper

Electronic supplementary material The online version of this article (doi:10.1007/s12678-017-0403-9) contains supplementary material, which is available to authorized users.

✉ Wang Gao
wgao@jlu.edu.cn

✉ Timo Jacob
timo.jacob@uni-ulm.de

[1] Key Laboratory of Automobile Materials (Jilin University), Ministry of Education, and School of Materials Science and Engineering, Jilin University, Changchun 130022, China

[2] Institut für Elektrochemie, Universität Ulm, Albert-Einstein-Allee 47, 89081 Ulm, Germany

Introduction

With a growing energy demand and fast depletion of fossil fuels, it is urgent to find new energy sources. One potential approach is to fix atmospheric CO_2 into value-added products using renewable power sources without additional CO_2 generation, such as solar source, wind, and tidal energy [1, 2]. Formation of oxygenated compounds, such as methanol, ethanol, and formic acid from CO_2 reduction, has been intensively investigated in view of their added value [3]. Especially the formation of methanol has drawn much attention because of its minimum hydrogen requirement and its large demand as a bulk chemical [2, 4–7].

Among C1 chemicals, methanol is one of the species most widely used in various chemical applications [8]. It can be used as a clean synthetic fuel additive and is considered as an alternative fuel source. It is a better and cleaner automobile fuel with a high octane number and with lower emissions of NO_x, ozone, CO, and aromatic vapors compared to other fossil fuels. Methanol is also a convenient hydrogen carrier for PEM fuel cells. In addition, it is a main building block for the production of other important chemicals, such as olefins and aromatics [9, 10]. Commercially, methanol is produced from synthesis gas ($CO/CO_2/H_2$) mainly over copper/zinc catalysts [11–16]. In this system, the methanol synthesis reaction, the water-gas shift reaction (WGS) [17, 18], and the reverse water-gas shift (rWGS) [5, 19, 20] reaction take place simultaneously:

$$CO_2 + 3\,H_2 \rightarrow CH_3OH + H_2O \quad (1)$$

$$H_2O + CO \leftrightarrows H_2 + CO_2 \quad (2)$$

There have been extensive investigations on copper-based catalysts, and it is well accepted that copper is the active center [15, 16, 21–24]. However, recently, some studies have indicated that the Zn/ZnO substrate has an essential effect on the reaction, which can improve the performance of catalysts to some extent [5, 25–29]. Although the effective sites have been studied thoroughly, there is still some debate on their exact nature. As the focus of our studies is on the catalytic reaction as well as the influence of co-adsorbated water on the mechanism of methanol formation, here we concentrate on the pure Cu metal. It was found that the activity of Cu(211) for CO_2 as well as for CO hydrogenation is more advanced than on Cu(111) [25, 30]. Moreover, carbon-labeling experiments have shown that CO_2 is the major reactant under industrial conditions [12, 20, 31, 32]. In addition, ^{13}C-labeling experiments indicated that methanol was generated exclusively from the adsorbed CH_2O* intermediate and not from the adsorbed surface formate [33].

Great efforts have been spent to explore the exact reaction mechanisms of CO_2 hydrogenation [24, 34–39], but yet no complete consensus of the pathways has been achieved. Traditionally, two possible reaction mechanisms have been proposed. One is the direct hydrogenation of CO_2 into HCOO (formate) [24, 25, 38]. Yang et al. have shown that it would be hydrogenated into H_2COO (dioxomethylene), followed by the formation of H_2CO (formaldehyde) [36]. In contrast, Studt et al. proposed that HCOO would first form HCOOH, followed by the formation of H_2COOH. Then, the H_2COOH is converted to H_2CO and OH [40]. Along the alternative reaction mechanism, CO_2 first reacts to CO through an OCOH intermediate, and the following CO hydrogenation can proceed through CHO or COH intermediates [37–42]. In case CHO is formed, CH_2O will also be present as an intermediate. In most studies, it is stated that once CH_2O is formed, the next protonation product is CH_3O [25, 38, 43–45]. In fact, this step can again follow different reaction pathways, e.g., the formation of CH_2OH with an O–H bond formed. Ye et al. have studied the formation of CH_2OH from CH_2O on In_2O_3(110), but found it energetically less favorable than the formation of CH_3O [34]. Although many studies have already addressed the reaction mechanism, there still exists a controversy on the exact pathways, which has been the main motivation of the present work.

CO_2 reduction experiments demonstrated that under variable reaction conditions, water does play different roles. With Cu as an effective catalyst, the main products for the electrochemical reduction of CO_2 in an aqueous electrolyte are CH_4, C_2H_4, and HCOOH, while under gaseous conditions, CH_3OH will form as the main product [5, 25, 46]. Montoya et al. found that without the charged water layer at the metal surface, the formation of CO dimers is prohibitively endergonic [47]. In other words, water in the electrochemical interface may accelerate the reaction to some extent. In contrast, it was found that water molecules that are formed during the reaction might suppress the formation of CH_3OH from syngas [17, 32]. Here, one explanation is that these water molecules block active copper sites and thus inhibit the adsorption of CO_2 for the follow-up reactions [17]. On the other hand, it was argued that these water molecules accelerate the crystallization of Cu and ZnO, resulting in the catalyst's deactivation [48]. Notably, the latter explanation implies that crystallization of Cu and ZnO leads to a decrease in surface area, being consistent with the former explanation that water molecules can block active copper sites. Further, Zhao et al. have studied the effect of H_2O on this reaction, finding that H_2O plays an inhibiting role in the hydrogenation of HCOO into methanol in the formate pathway [44]. However, in their studies, only a single water molecule was introduced, which is insufficient to mimic the catalyst surface under aqueous conditions. Thus, further studies are required to understand the effect of co-adsorbed water on the reaction process.

In our work, a detailed reaction scheme has been sketched for the conversion of syngas with CO/CO_2 hydrogenation as the initial step on a Cu(211) electrocatalyst. We propose a feasible reaction route for methanol formation with the reactive intermediate CH_2O* [33], which proceeds via the reaction sequence $CO^* \rightarrow CHO^* \rightarrow CH_2O^* \rightarrow CH_2OH^* \rightarrow CH_3OH^*$. We further elucidate the effect of water molecules produced along the synthesis process, finding that they are indeed capable of reducing the catalyst's activity [17, 32, 48]. Therefore, these results are helpful in understanding the CH_3OH formation mechanism and the essence of H_2O affecting the reaction process.

Method

All theoretical data were obtained using the CASTEP code with ultrasoft pseudopotentials and the generalized gradient approximation (GGA) exchange-correlation functional proposed by Perdew, Burke, and Ernzerhof (PBE) combined with the TSsurf dispersion corrections [49–52]. This is motivated by the fact that while PBE alone is known to overestimate binding energies for adsorption processes on transition-metal surfaces [52–54], it had been demonstrated that the inclusion of entropy and thermochemical contributions as well as van der Waals (vdW) forces yields an improved description of the CO_2 hydrogenation [40, 43, 55]. We adopted a plane wave basis set with an energy cutoff of 400 eV, and used a $2 \times 2 \times 1$ Monkhorst-Pack *k*-point scheme for the Brillouin zone sampling. All calculations were performed on the Cu(211) surface orientation with five layer slabs, where the bottom three layers were fixed at the bulk-truncated structure, leaving the top two surface layers and the adsorbents as well as co-adsorbed water to be fully relaxed. The periodic images of the slab were

separated by a vacuum gap being at least 15 Å wide. To investigate the reaction pathways, the transition state (TS) search procedure as implemented in the CASTEP code was used, which employs a combination of linear and quadratic synchronous transit (LST/QST) algorithms with subsequent conjugate gradient methods [56].

We define adsorption energy (E_{ads}) of the molecules as follows:

$$E_{ads} = (E_{total} - E_{substrate} - n \cdot E_{molecule})/n, \quad (3)$$

where E_{total} is the total energy of the complete system (surface + adsorbates), $E_{substrate}$ is the energy of the substrate (i.e., slab only), and $n \cdot E_{molecule}$ is the total energy of a single molecule ($E_{molecule}$) multiplied by the number of molecules (n) in the unit cell.

Results and Discussion

Cu(211) With and Without H_2O Chain

Motivated by previous studies on representative Cu surfaces [25], we have chosen Cu(211) as model surface (see Fig. 1a), which combines terrace and step edge features, for calculating the thermodynamic and kinetic parameters for each elementary step. It was also suggested that hydrogen-bonded water molecules can be easily accommodated at the edge of transition metal surfaces. Therefore, we adopted Cu(211) with H_2O chains to simulate the system under reaction conditions (where surface water had been formed by the reaction). Moreover, Site et al. have revealed that water adsorbs preferentially at step edges, forming linear clusters or chains, stabilized by the cooperative effect of chemical bonds with the substrate and hydrogen bonds, which additionally supports the rationality of our model [57]. Our calculations show that H_2O chains are formed on the step by alternating H bond lengths between 2.81, 2.66, and 2.83 Å (Fig. 1b). This combination of interactions leads to an adsorption energy of −0.66 eV/H_2O. Regarding the binding, it should be mentioned that due to similar high-frequency vibrational modes of water in the gas phase (3910 and 3796 cm^{-1}) and after adsorption (3801 and 3538 cm^{-1}), ZPE contributions to the adsorption energy of water are very small. Therefore, here, we only take the entropy contributions into account (0.38 eV for adsorbed H_2O molecule and 0.98 eV for free H_2O at 500K, 0.16 eV for adsorbed H_2O molecule and 0.58 eV for free H_2O at 298K), leading to an adsorption free energy (ΔG) of −0.06 eV/H_2O at 500 K and −0.24 eV/H_2O at 298 K on Cu(211), indicating that H_2O molecules can indeed be adsorbed on Cu(211). It seems that especially the presence of step edges at the Cu(211) surfaces is important to facilitate binding of water. In addition, the high pressure (50–100 bar) that is used for the formation of methanol industrially also facilitates the adsorption of H_2O molecules.

The calculated adsorption energies for the different molecules are summarized in Table 1. Obviously, the adsorption energy of CO_2, H_2, and CO is increased by 0.14, 0.07, 0.30 eV, respectively, under the influence of H_2O chains. It is well known that PBE misses long-range vdW force, which is ubiquitous in all materials. Moreover, vdW forces also play an essential role in the adsorption of other molecules (such as, H_2O and CH_3OH) and the reaction energies [40]. Thus, herein we adopted dispersion force corrections by using the PBE + TSsurf approach. The contribution of vdW interactions on the bare Cu(211) surface is up to −0.29 eV for the CO_2 molecule and −0.08 eV for H_2 molecule where the vdW forces are the decisive factor for adsorption of these molecules. Under the influence of water, the contribution of vdW interactions to the adsorption energy of CO_2 molecule changes to −0.31 eV and for the H_2 molecule to −0.14 eV, again showing the essential role of vdW interations in the binding. For the CH_3OH molecule, the vdW contribution to adsorption energy is larger than 0.30 eV with an adsorption energy −0.58 eV on Cu(211) and −0.87 eV in the presence of co-adsorbed water. In addition, the contribution of vdW interactions to the CO adsorption is increased by 0.16 eV in the presence of neighboring water. In our previous study we have identified that vdW contributions to the adsorption energy of CO on Cu(111) is up to 30% [55], whereas with the corrections of zero point energy, the pure PBE (−0.89) and the vdW corrected PBE (−1.15) all overestimate the CO adsorption energy compared to an experimental value of −0.58 eV [58].

Overall, vdW interactions seem to have a significant effect on the adsorption energies of small molecules, especially when being only weakly adsorbed. This should additionally have an impact on reaction mechanisms, an aspect that will be elucidated in the next sections.

CHO*, CH_2O*, and CH_3O* Pathways

In the first step, different possible CO_2 reduction pathways on Cu(211) were studied without co-adsorbed water. Figure 2 shows the energy diagrams for different CH_3OH formation pathways, where they are denoted by the intermediate formed before the hydroxyl formation. For example, the CHO* pathway means that the CHOH* (hydroxymethylene) will be formed through the hydrogenation of CHO*. Similarly, the CH_2O* pathway means that the product of CH_2O* hydrogenation is CH_2OH* (hydroxymethyl), while the CH_3O* pathway involves the formation of CH_3OH* (methanol) by hydrogenation of CH_3O*.

CHO Pathway*

For the CHO* pathway, CO* hydrogenation proceeds via the hydrogenation of the carbon atom of CO*, following the

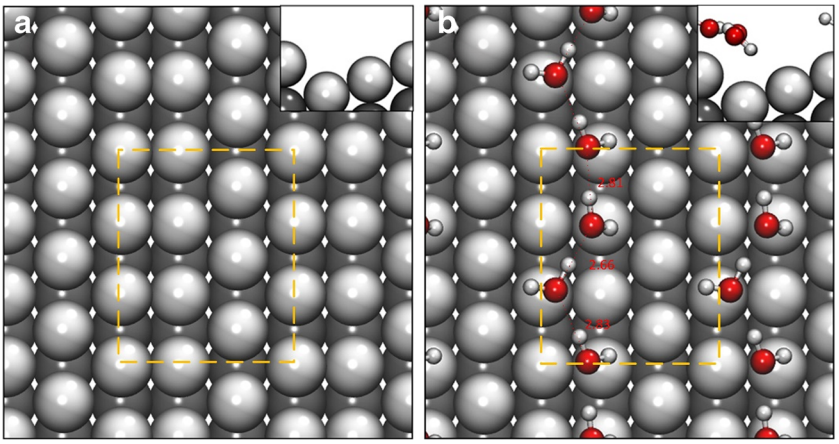

Fig. 1 **a** Bare Cu(211), **b** Cu(211) with H_2O chain. The *big white* and *black balls* represent the Cu atoms; the *small white balls* are H atoms, while the *red ones* are O atoms. *Insets* are side views of the corresponding interfaces

stepwise hydrogenation with the formation of CHO*, CHOH*, and CH_2OH* intermediates. Lastly, CH_2OH* is hydrogenated into CH_3OH. The formation of CHO* from CO* is an endothermic process (reaction energy $E_r = 0.70$ eV) with an energy barrier of $E_a = 1.05$ eV, which is consistent with the results of Asthagiri et al. ($E_r = 0.71$ eV and $E_a = 1.03$ eV) [45]. The hydroxyl formation (CHOH*) is the determining step for this pathway, which is endothermic by 0.18 eV with a barrier of 1.38 eV. Then, CHOH* can be further hydrogenated into CH_2OH* with a relatively small barrier of 0.61 eV and an overall energy gain of $E_r = -0.71$ eV. The final hydrogenation step, the formation of CH_3OH, releases 1.09 eV and has a barrier of 0.71 eV, which is higher than the barrier reported by Mavrikakis et al. ($E_a = 0.51$ eV) [42].

CH_2O Pathway*

For this pathway, the formation of CHO* proceeds as already described for the CHO* pathway. The difference in both mechanisms stems from the process of CHO* hydrogenation. Along the CHO* pathway, the hydrogenation of CHO* leads to the formation of CHOH*, and now, it leads to the formation of CH_2O*. The latter process, i.e., the CH_2O* formation, is exothermic by 0.48 eV with a barrier of 0.63 eV, matching well with the results of Asthagiri et al. ($E_a = 0.60$ eV) [45]. Compared to the process of CHOH* formation ($E_a = 1.38$ eV and $E_r = 0.18$ eV), the formation of CH_2O* is more favorable both kinetically and thermodynamically. In the following, there is a configuration transformation of CH_2O*, which in Fig. 2 we labeled as the transfer from CH_2O*-1 to CH_2O*-2, a process being associated with a small energy change of $E_r = -0.04$ eV. As shown in Fig. 3, the CH_2O*-1 and CH_2O*-2 molecules are adsorbed at the step edge of the Cu surface, but the O atoms point at different directions. The next step is the formation of CH_2OH*, which is exothermic by 0.35 eV with a barrier of 0.95 eV. After the formation of CH_2OH*, the remaining step of CH_3OH* formation is consistent with the CHO* pathway. For the CH_2O* pathway, the determining step is the formation of CHO* ($E_a = 1.05$ eV and $E_r = 0.70$ eV). Thus, comparing the determining step of CHOH* formation for both pathways indicates a preference for the CH_2O* reaction mechanism.

Table 1 Adsorption energies, E_{ad}, in electron volts, of different molecules on bare Cu(211) and Cu(211) with a H_2O chain using the PBE and PBE + TSsurf approximations

System	E_{ad} (eV)	CO_2*	H_2*	CO*	CH_3OH*
Cu(211)	PBE + TSsurf	−0.22	−0.06	−1.01	−0.58
	PBE	0.07	0.02	−0.81	−0.25
	vdW	−0.29	−0.08	−0.20	−0.33
Cu(211) with H_2O chain	PBE + TSsurf	−0.36	−0.13	−1.31	−0.87
	PBE	−0.05	0.01	−0.95	−0.55
	vdW	−0.31	−0.14	−0.36	−0.32

CH_3O Pathway*

The difference between the CH_2O* and the CH_3O* pathways is that the stepwise hydrogenation of CH_2O* to CH_3OH* is through CH_3O* (CH_3O* pathway) or its isomer CH_2OH* (CH_2O* pathway). In both mechanisms, the formation of CH_3OH* is from CH_2O* where one C–H and one O–H bonds need to be formed. Along the CH_2O* pathway, the O–H bond is formed first, followed by the formation a C–H bond, while the order is the opposite for the CH_3O* pathway. Here, the process of CH_2O* hydrogenation into CH_3O* is very facile with a barrier of only 0.38 eV and an exothermicity of 0.97 eV, which coincides well with the results of Li et al. ($E_a = 0.35$ eV and $E_r = -0.92$ eV) [59]. Compared to the process of CH_2OH* formation ($E_a = 0.95$ eV and $E_r = -0.35$ eV), the formation of CH_3O* from CH_2O* seems more favorable. However, the CH_3OH* formation from CH_3O* (being the determining step) is kinetically prohibitive, which must overcome a barrier of 1.32 eV, which is 0.15 eV higher than the value obtained by Mavrikakis et al. [42]. Thus, considering all the elementary steps, the CH_2O* pathway seems more promising than the CH_3O* pathway.

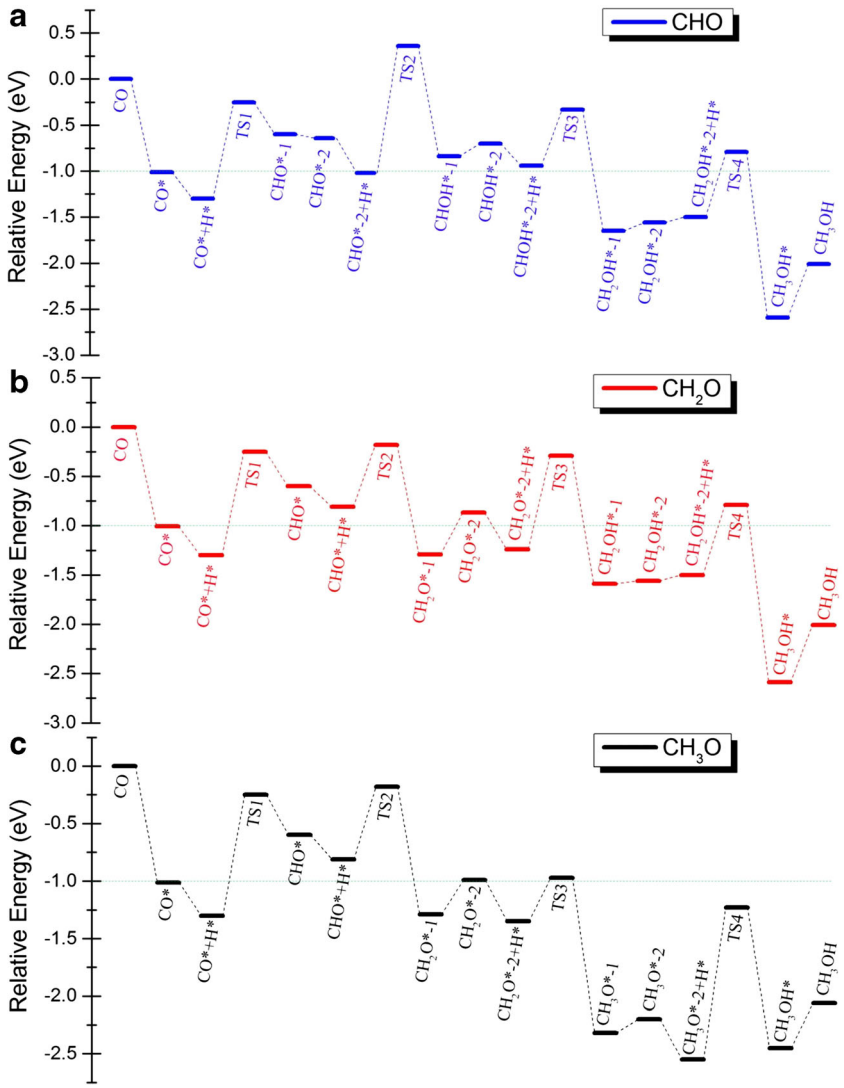

Fig. 2 **a**–**c** Energy diagrams of different CH_3OH* formation pathways on bare Cu(211)

In the three considered reaction sequences, the most promising one is the CH_2O* pathway, of which the determining step is the formation of CHO*. The process of this pathway proceeds as CO* → CHO* → CH_2O* → CH_2OH* → CH_3OH* and the reactive intermediate is CH_2O*. The isotope labeling study for methanol synthesis on Cu/ZrO_2 suggested that CH_3OH is exclusively formed from CH_2O* (not HCOO*), which agrees well with our results [33].

As stated above, in the present work, we concentrated on the role of water on the reaction mechanism and did not explicitly take zero-point energy and entropy corrections into account. Although this approach seems to be sufficient for such a comparative study, our absolute reaction energies (ΔE) for the overall CH_3OH formation are all about −2.0 eV, which is higher than the experimental value [60]. This difference is mainly associated with the separated (not adsorbed) molecules as the following estimation shows. While the zero point energy contributions are 0.14 eV for CO and 1.35 eV for CH_3OH [61], taking these contributions into account, we would obtain the overall reaction free energy to be 0.80 eV, which is relatively close to the experimental value of 0.95 eV [60]. The remaining differences might certainly be attributed to the omitting of ΔpV contributions to the enthalpy.

Influence of a Co-adsorbed H_2O Chain

To verify the effect of co-adsorbed water, we have calculated the same reaction pathways on Cu(211) in the presence of a co-adsorbed H_2O chain (Fig. S2 and Table S3). The results reveal that due to water the barriers for CHO* and CH_3OH* formation along the CHO* pathway increase by 0.08 and 0.14 eV, respectively. For the CH_2O* pathway, the reaction barrier of each step is also increased by up to 0.34 eV (for the CH_2OH* formation). Along the CH_3O* pathway, the barriers of the former two steps increase by the same values as in the CH_2O* pathway. However, the CH_3O* and CH_3OH* formation steps now have barriers that are increased by 0.41 and 0.03 eV in the presence of water. Meanwhile, the reaction

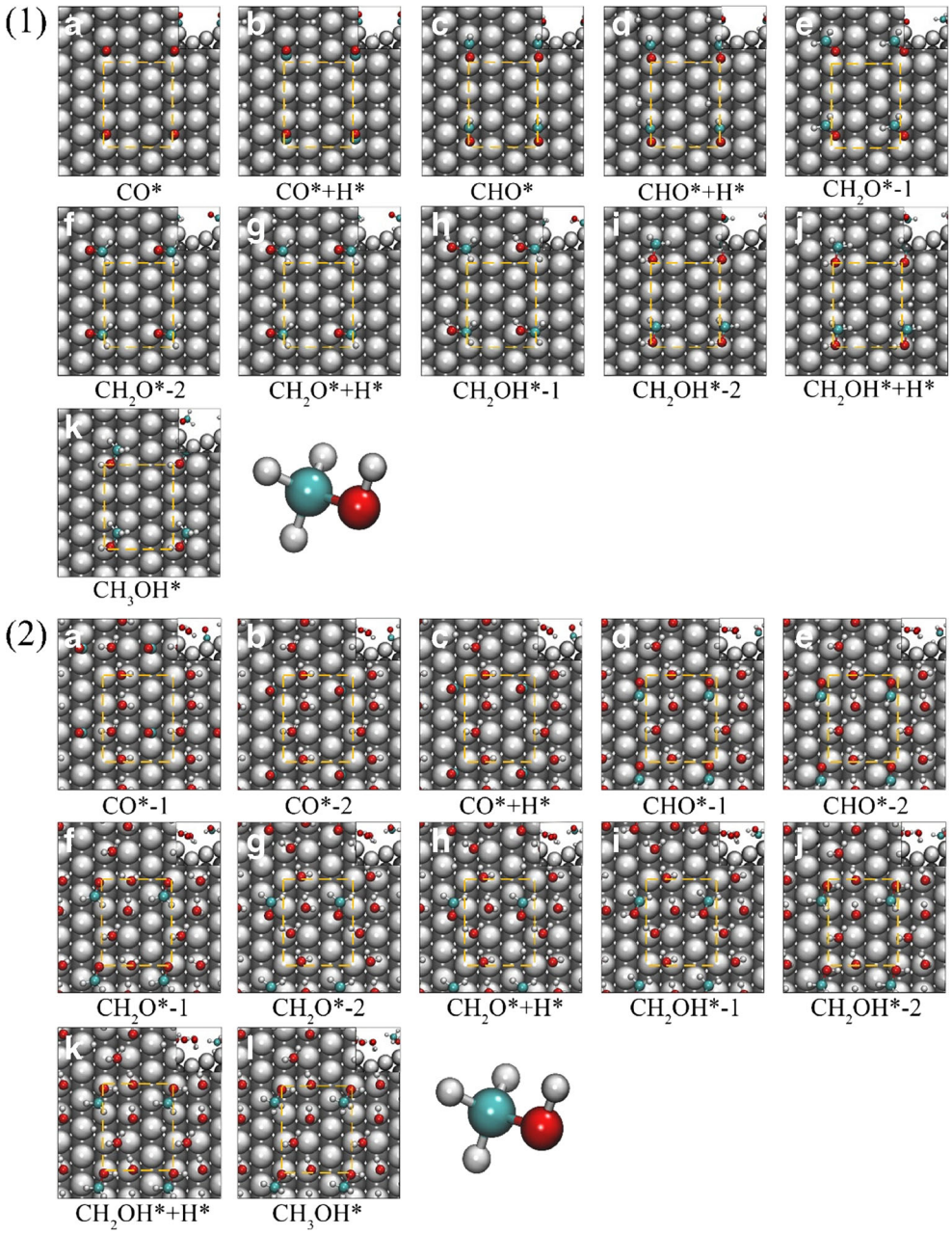

Fig. 3 Configuration details of the CH_2O^* reaction pathway on Cu(211) without water (*1*) and with a co-adsorbed water chain (*2*)

$CH_3O^* + H^* \rightarrow CH_3OH^*$ qualitatively changes from an endothermic process (E_r = 0.10 eV) to an exothermic process (E_r = −0.18 eV), but the larger barrier (1.35 eV) indicates that this step is prohibited dynamically. All the results indicate that the co-adsorbed H_2O chain apparently suppresses this reaction, which is consistent with the experimental results that water molecules have an inhibiting effect [17, 32, 48].

Now, we discuss how water influences the overall reaction mechanisms. The energy diagram of Fig. S2 shows that with water, the CH_2O^* pathway is still the most effective reaction mechanism. Without water, the CO* molecule adsorbs at a step site of the (211) surface vertically through its C atom (Fig. 3 1a). In the presence of H_2O, the CO moves to the (111) terrace (Fig. 3 1a) as the H_2O chain occupies and blocks the step. Without water, CHO* adsorbed through their C and O atoms "lying" on the step, while the hydrogen atom pointed into the vacuum. Under the influence of the H_2O chain, the adsorption configuration of CHO* did not change but was pushed to the terrace. CH_2O^* and CH_2OH^* intermediates are also shifted to the (111) terrace in the presence of water while again their configurations (all the atoms parallel to the surface) did not alter. Due to the presence of the H_2O chain in the system, the adsorption sites of the intermediates have been pushed from the active step to the less active terrace. In addition, there are interactions between the intermediates (CH_2O^*, CH_2OH^*) with the co-adsorbed H_2O molecules through H

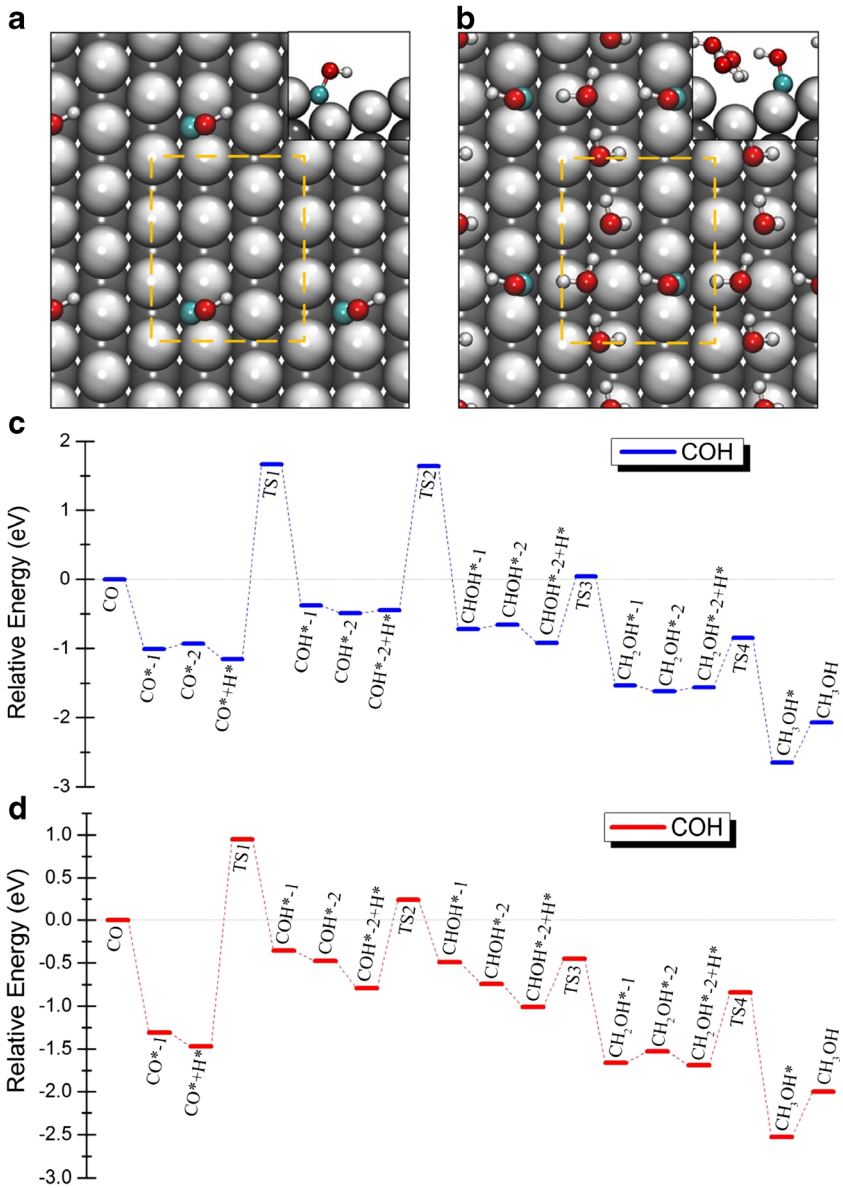

Fig. 4 COH* intermediate configuration on **a** bare Cu(211) and **b** Cu(211) with a H_2O chain. Energy diagram of the COH* pathway on **c** bare Cu(211) and **d** Cu(211) with a H_2O chain

bonds, which in addition affect the molecular orientations. On one hand, these interactions lead to an increase of the adsorption energies of the intermediates and, on the other hand, result in increased activation barriers and thus lower activities. Therefore, our studies clearly show that the presence of water will certainly influence the adsorption sites and configurations of the intermediates.

Role of the vdW Forces

To explain the influence of vdW interactions on the reaction mechanisms, we analyzed the reaction barriers and energies of main steps for the CHO*/CH_2O*/CH_3O* pathways (Table S4) both on bare Cu(211) and Cu(211) with the H_2O chain. For the CHO* pathway on bare Cu(211), the contribution of vdW forces to the reaction energy is up to 0.11 eV (18.6%; the percentage is the ratio of the vdW contribution to the overall energies) for the CO* + H* → CHO* step, where the contribution to the barrier is 0.11 eV (11.7%). The corresponding contribution in the CH_2O* mechanism increases to 20.7% for the CH_2OH* formation process. For the CH_3O*, formation step along the CH_3O* pathway, vdW contributions are even 26.7% on Cu(211). Under the influence of water, the vdW contributions further increase to 20, 30.8, and 52.6% for CHO*, CH_2O*, and CH_3O* pathways, respectively. It can be seen that due to the presence of water in the system, the contribution of the vdW forces has been increased significantly.

Overall, we find a preference for the CH_2O* pathway, a result that differs from the pathway suggested by Nørskov et al. [40], who found a preference for a CO* → CHO* → CH_2O* → CH_3O* → CH_3OH* sequence, which corresponds

to our CH_3O* pathway. However, in their work, the BEEF-vdW approach was employed to describe the vdW force, while the TSsurf method has been used in our work. The previous studies have found that the TSsurf method is applicable to metal surfaces where more precise results can be obtained compared to the other vdW schemes [52]. The significant contribution of vdW interactions to the reaction pathways can effectively change the selectivity of different pathways.

COH* and HCOO* Pathways

All reaction pathways that we have discussed so far are initiated with the hydrogenation of CO* into CHO* and a corresponding C–H bond formation. The other possible reaction pathways can proceed via O–H bond formation with CO* hydrogenation into COH* as the first step. In this case, the formation of the hydroxyl is at the first hydrogenation step, and all the remaining steps include the formation of C–H bonds. The reaction pathway proceeds as CO* → COH* → CHOH* → CH_2OH* → CH_3OH*. We excluded this pathway on Cu(211), because the first step, associated with CO* hydrogenation into COH*, is on one side kinetically hindered due to a high energy barrier of 2.83 eV and on the other side thermodynamically disadvantageous (E_r = 0.78 eV) (see Fig. 4c). As shown in Fig. 4a, COH* adsorbs vertically on Cu(211) with its C atom, while the O–H bond orients parallel to the surface. The next step of CHOH* formation from COH* must overcome a high barrier of 2.09 eV. Although being an exothermic step (E_r = −0.27 eV), the high barrier makes it kinetically hindered [44]. The high energy barriers of these two steps lead to a very low probability of this pathway to occur. In order to evaluate the influence of H_2O molecules, we also studied this pathway on Cu(211) with the H_2O chain. Due to the H_2O molecules, the barriers of the first two steps decrease by 0.41 and 1.06 eV, respectively, and both steps become endothermic. Therefore, considering the high barriers for the initial reaction steps, the COH* pathway is expected not to be relevant.

As stated before, CH_3OH* can also be formed directly from CO_2*. Here, two different pathways have been proposed; one proceeds via the sequence CO_2* → HCOO* → H_2COO* → H_2CO* and the other CO_2* → HCOO* → HCOOH* → H_2CO* [24, 25, 36, 38, 40]. The remaining steps to CH_3OH* are equivalent to the mechanism discussed previously for the CO* hydrogenation. As for both proposed pathways the first step is the formation of HCOO* from CO_2*, we calculated this process on Cu(211) with and without water. On bare Cu(211), this step is exothermic by −0.83 eV but requires overcoming a high barrier of 1.64 eV. In the presence of water, the barrier further increases even up to 2.98 eV and the exothermicity decreases to −0.33 eV. Although thermodynamically slightly preferred, again it seems kinetically hindered due to this high barrier. Therefore, it seems appropriate to disregard the direct CO_2* pathways for the present reaction process.

Conclusion

In conclusion, we have performed detailed studies on the formation of CH_3OH* on Cu(211), summarized in Scheme 1, and found that the most possible pathway proceeds via the reaction sequence CO* → CHO* → CH_2O* → CH_2OH* → CH_3OH*, in which the active intermediate of CH_2O* is in accord with experiments. We also found that the presence of co-adsorbed water at the preferred edge sites (represented as a H_2O chain) has an inhibiting effect on the CO_2 hydrogenation, which is again consistent with the experimental results. This suppression mainly stems from the effect of H bonds and vdW interactions. The H bonds induced by the H_2O chain change the orientation of the intermediates and increase their stabilities as well as the reaction barriers. The vdW contributions also lead to an

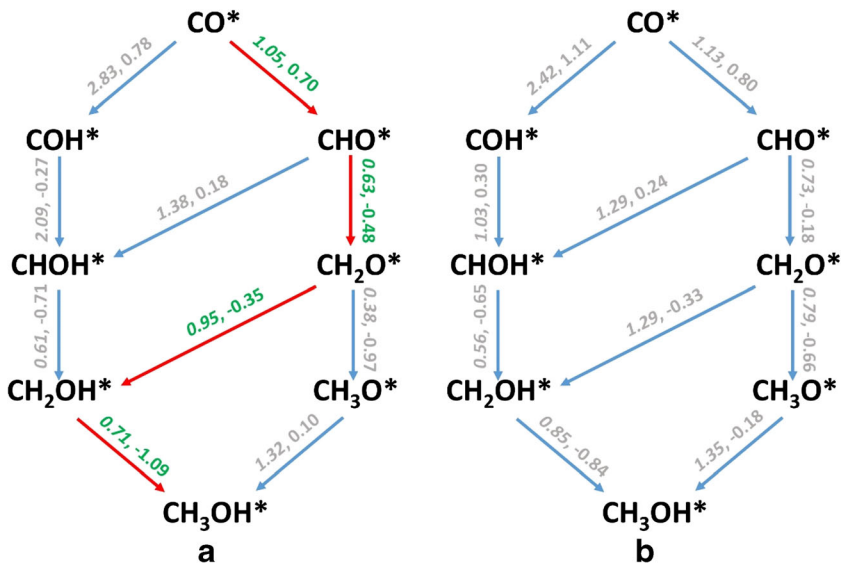

Scheme 1 Reaction pathways with the corresponding energies. Non-italic numbers are energy differences, while italic numbers are barriers. All energies are in electron volts. (**a**) reaction pathways on bare Cu(211) and (**b**) reaction pathways on Cu(211) with the co-adsorbed H_2O chain. The red arrows represent the most promising pathway

increase of the adsorption energies of intermediates and the correlated energy barriers for further reaction steps. Our results provide a comprehensive understanding of the mechanism and conceptually explain the experimental phenomenon (the inhibiting effect of H_2O molecules).

Acknowledgements The authors acknowledge support from the Deutsche Forschungsgemeinschaft (DFG) through the grant proposal (JA1072/9-1 and 9-2), which was part of the research unit DFG-FOR1376. Further, support by the Program for Thousand Young Talents Plan and the National Natural Science Foundation of China (No. 21673095, 51631004), the computing resources of High Performance Computing Center of Jilin University, and National Supercomputing Center in Jinan and in Shenzhen China are acknowledged. Finally, the authors also acknowledge the computer time supported by the state of Baden-Württemberg through the bwHPC project and the DFG through grant number INST40/467-1 FUGG.

References

1. E.V. Kondratenko, G. Mul, J. Baltrusaitis, G.O. Larrazabal, J. Perez-Ramirez, Status and perspectives of CO_2 conversion into fuels and chemicals by catalytic, photocatalytic and electrocatalytic processes. Energy Environ. Sci. **6**, 3112–3135 (2013)
2. K.C. Waugh, Methanol synthesis. Catal. Today **15**, 51–75 (1992)
3. K.P. Kuhl, E.R. Cave, D.N. Abram, T.F. Jaramillo, New insights into the electrochemical reduction of carbon dioxide on metallic copper surfaces. Energy Environ. Sci. **5**, 7050–7059 (2012)
4. F. Studt, I. Sharafutdinov, F. Abild-Pedersen, C.F. Elkjær, J.S. Hummelshøj, S. Dahl, I. Chorkendorff, J.K. Nørskov, Discovery of a Ni-Ga catalyst for carbon dioxide reduction to methanol. Nat. Chem. **6**, 320–324 (2014)
5. J. Graciani, K. Mudiyanselage, F. Xu, A.E. Baber, J. Evans, S.D. Senanayake, D.J. Stacchiola, P. Liu, J. Hrbek, J.F. Sanz, J.A. Rodriguez, Highly active copper-ceria and copper-ceria-titania catalysts for methanol synthesis from CO_2. Science **345**, 546–550 (2014)
6. O. Martin, A.J. Martín, C. Mondelli, S. Mitchell, T.F. Segawa, R. Hauert, C. Drouilly, D. Curulla-Ferré, J. Pérez-Ramírez, Indium oxide as a superior catalyst for methanol synthesis by CO_2 hydrogenation. Angew. Chem. Int. Ed. **55**, 1–16 (2016)
7. E.E. Barton, D.M. Rampulla, A.B. Bocarsly, Selective solar-driven reduction of CO_2 to methanol using a catalyzed p-GaP based photoelectrochemical cell. J. Am. Chem. Soc. **130**, 6342–6344 (2008)
8. L.V. MacDougall, Methanol to fuels routes—the achievements and remaining problems. Catal. Today **8**, 337–369 (1991)
9. L.K. Rihko-Struckmann, A. Peschel, R. Hanke-Rauschenbach, K. Sundmacher, Assessment of methanol synthesis utilizing exhaust CO_2 for chemical storage of electrical energy. Ind. Eng. Chem. Res. **49**, 11073–11078 (2010)
10. G.A. Olah, Beyond oil and gas: The methanol economy. Angew. Chem. Int. Ed. **44**, 2636–2639 (2005)
11. J.D. Grunwaldt, A.M. Molenbroek, N.Y. Topsøe, H. Topsøe, B.S. Clausen, In situ investigations of structural changes in Cu/ZnO catalysts. J. Catal. **194**, 452–460 (2000)
12. M. Muhler, E. Törnqvist, L.P. Nielsen, B.S. Clausen, H. Topsøe, On the role of adsorbed atomic oxygen and CO_2 in copper based methanol synthesis catalysts. Catal. Lett. **25**, 1–10 (1994)
13. P.L. Hansen, J.B. Wagner, S. Helveg, J.R. Rostrup-Nielsen, B.S. Clausen, H. Topsøe, Atom-resolved imaging of dynamic shape changes in supported copper nanocrystals. Science **295**, 2053–2055 (2002)
14. X. Dong, H.-B. Zhang, G.-D. Lin, Y.-Z. Yuan, K.R. Tsai, Highly active CNT-promoted cu-ZnO-Al_2O_3 catalyst for methanol synthesis from $H_2/CO/CO_2$. Catal. Lett. **85**, 237–246 (2003)
15. J.S. Lee, K.I. Moon, S.H. Lee, S.Y. Lee, Y.G. Kim, Modified Cu/ZnO/Al_2O_3 catalysts for methanol synthesis from CO_2/H_2 and CO/H_2. Catal. Lett. **34**, 93–99 (1995)
16. F. Liao, Y. Huang, J. Ge, W. Zheng, K. Tedsree, P. Collier, X. Hong, S.C. Tsang, Morphology-dependent interactions of ZnO with Cu nanoparticles at the materials' interface in selective hydrogenation of CO_2 to CH_3OH. Angew. Chem. Int. Ed. **50**, 2162–2165 (2011)
17. O.-S. Joo, K.-D. Jung, I. Moon, A.Y. Rozovskii, G.I. Lin, S.-H. Han, S.-J. Uhm, Carbon dioxide hydrogenation to form methanol via a reverse-water-gas-shift reaction (the CAMERE process). Ind. Eng. Chem. Res. **38**, 1808–1812 (1999)
18. K.M.V. Bussche, G.F. Froment, A steady-state kinetic model for methanol synthesis and the water gas shift reaction on a commercial Cu/ZnO/Al_2O_3 catalyst. J. Catal. **161**, 1–10 (1996)
19. E.L. Kunkes, F. Studt, F. Abild-Pedersen, R. Schlögl, M. Behrens, Hydrogenation of CO_2 to methanol and CO on Cu/ZnO/Al_2O_3: Is there a common intermediate or not? J. Catal. **328**, 43–48 (2015)
20. J. Yoshihara, C.T. Campbell, Methanol synthesis and reverse water–gas shift kinetics over Cu(110) model catalysts: structural sensitivity. J. Catal. **161**, 776–782 (1996)
21. G.C. Chinchen, K.C. Waugh, D.A. Whan, The activity and state of the copper surface in methanol synthesis catalysts. Appl. Catal. **25**, 101–107 (1986)
22. P.B. Rasmussen, M. Kazuta, I. Chorkendorff, Synthesis of methanol from a mixture of H_2 and CO_2 on Cu(100). Surf. Sci. **318**, 267–280 (1994)
23. J. Nakamura, Y. Choi, T. Fujitani, On the issue of the active site and the role of ZnO in Cu/ZnO methanol synthesis catalysts. Top. Catal. **22**, 277–285 (2003)
24. Y. Yang, J. Evans, J.A. Rodriguez, M.G. White, P. Liu, Fundamental studies of methanol synthesis from CO_2 hydrogenation on Cu(111), Cu clusters, and Cu/ZnO(0001). Phys. Chem. Chem. Phys. **12**, 9909–9917 (2010)
25. M. Behrens, F. Studt, I. Kasatkin, S. Kühl, M. Hävecker, F. Abild-Pedersen, S. Zander, F. Girgsdies, P. Kurr, B.-L. Kniep, M. Tovar, R.W. Fischer, J.K. Nørskov, R. Schlögl, The active site of methanol synthesis over Cu/ZnO/Al_2O_3 industrial catalysts. Science **336**, 893–897 (2012)
26. S. Kuld, M. Thorhauge, H. Falsig, C.F. Elkjær, S. Helveg, I. Chorkendorff, J. Sehested, Quantifying the promotion of Cu catalysts by ZnO for methanol synthesis. Science **352**, 969–974 (2016)
27. S.A. Kondrat, P.J. Smith, P.P. Wells, P.A. Chater, J.H. Carter, D.J. Morgan, E.M. Fiordaliso, J.B. Wagner, T.E. Davies, L. Lu, J.K. Bartley, S.H. Taylor, M.S. Spencer, C.J. Kiely, G.J. Kelly, C.W. Park, M.J. Rosseinsky, G.J. Hutchings, Stable amorphous georgeite as a precursor to a high-activity catalyst. Nature **531**, 83–87 (2016)
28. R. van den Berg, G. Prieto, G. Korpershoek, L.I. van der Wal, A.J. van Bunningen, S. Lægsgaard-Jørgensen, P.E. de Jongh, K.P. de Jong, Structure sensitivity of Cu and CuZn catalysts relevant to industrial methanol synthesis. Nat. Commun. **7**, 13057 (2016)
29. S. Kattel, P.J. Ramírez, J.G. Chen, J.A. Rodriguez, P. Liu, Active sites for CO_2 hydrogenation to methanol on cu/ZnO catalysts. Science **355**, 1296–1299 (2017)
30. W. Janse van Rensburg, M.A. Petersen, M.S. Datt, J.-A. den Berg, P. Helden, On the kinetic interpretation of DFT-derived energy profiles: Cu-catalyzed methanol synthesis. Catal. Lett. **145**, 559–568 (2014)
31. G.C. Chinchen, P.J. Denny, D.G. Parker, M.S. Spencer, D.A. Whan, Mechanism of methanol synthesis from $CO_2/CO/H_2$ mixtures over copper/zinc oxide/alumina catalysts: use of ^{14}C-labelled reactants. Appl. Catal. **30**, 333–338 (1987)
32. Y. Yang, C.A. Mims, D.H. Mei, C.H.F. Peden, C.T. Campbell, Mechanistic studies of methanol synthesis over Cu from CO/CO_2/

H_2/H_2O mixtures: The source of C in methanol and the role of water. J. Catal. **298**, 10–17 (2013)
33. E.E. Ortelli, J.M. Weigel, A. Wokaun, Methanol synthesis pathway over Cu/ZrO_2 catalysts: a time-resolved D RIFT ^{13}C-labelling experiment. Catal. Lett. **54**, 41–48 (1998)
34. J. Ye, C. Liu, D. Mei, Q. Ge, Active oxygen vacancy site for methanol synthesis from CO_2 hydrogenation on $In_2O_3(110)$: a DFT study. ACS Catal. **3**, 1296–1306 (2013)
35. J. Kiss, J. Frenzel, N.N. Nair, B. Meyer, D. Marx, Methanol synthesis on ZnO(0001). III. Free energy landscapes, reaction pathways, and mechanistic insights. J. Chem. Phys. **134**, 064710 (2011)
36. Y. Yang, M.G. White, P. Liu, Theoretical study of methanol synthesis from CO_2 yydrogenation on metal-doped Cu(111) surfaces. J. Phys. Chem. C **116**, 248–256 (2012)
37. Y.-F. Zhao, R. Rousseau, J. Li, D. Mei, Theoretical study of syngas hydrogenation to methanol on the polar Zn-terminated ZnO(0001) surface. J. Phys. Chem. C **116**, 15952–15961 (2012)
38. C. Liu, P. Liu, Mechanistic study of methanol synthesis from CO_2 and H_2 on a modified model Mo_6S_8 cluster. ACS Catal. **5**, 1004–1012 (2015)
39. F. Studt, M. Behrens, E.L. Kunkes, N. Thomas, S. Zander, A. Tarasov, J. Schumann, E. Frei, J.B. Varley, F. Abild-Pedersen, J.K. Nørskov, R. Schlögl, The mechanism of CO and CO_2 hydrogenation to methanol over Cu-based catalysts. ChemCatChem **7**, 1105–1111 (2015)
40. F. Studt, F. Abild-Pedersen, J.B. Varley, J.K. Nørskov, CO and CO_2 hydrogenation to methanol calculated using the BEEF-vdW functional. Catal. Lett. **143**, 71–73 (2012)
41. Q.-L. Tang, Q.-J. Hong, Z.-P. Liu, CO_2 fixation into methanol at Cu/ZrO_2 interface from first principles kinetic Monte Carlo. J. Catal. **263**, 114–122 (2009)
42. L.C. Grabow, M. Mavrikakis, Mechanism of methanol synthesis on Cu through CO_2 and CO hydrogenation. ACS Catal. **1**, 365–384 (2011)
43. A.J. Medford, J. Sehested, J. Rossmeisl, I. Chorkendorff, F. Studt, J.K. Nørskov, P.G. Moses, Thermochemistry and micro-kinetic analysis of methanol synthesis on ZnO (0001). J. Catal. **309**, 397–407 (2014)
44. Y.-F. Zhao, Y. Yang, C. Mims, C.H.F. Peden, J. Li, D. Mei, Insight into methanol synthesis from CO_2 hydrogenation on Cu(1 1 1): Complex reaction network and the effects of H_2O. J. Catal. **281**, 199–211 (2011)
45. X. Nie, W. Luo, M.J. Janik, A. Asthagiri, Reaction mechanisms of CO_2 electrochemical reduction on Cu(111) determined with density functional theory. J. Catal. **312**, 108–122 (2014)
46. Y. Hori, in *In Modern aspects of electrochemistry*, ed. by C. Vayenas, R. White, M. Gamboa-Aldeco. Electrochemical CO_2 reduction on metal electrodes (Springer, New York, 2008), pp. 89–189
47. J.H. Montoya, C. Shi, K. Chan, J.K. Nørskov, Theoretical insights into a CO dimerization mechanism in CO_2 electroreduction. J. Phys. Chem. Lett. **6**, 2032–2037 (2015)
48. J. Wu, M. Saito, M. Takeuchi, T. Watanabe, The stability of Cu/ZnO-based catalysts in methanol synthesis from a CO_2-rich feed and from a CO-rich feed. Appl. Catal. A-Gen. **218**, 235–240 (2001)
49. M.D. Segall, J.D.L. Philip, M.J. Probert, C.J. Pickard, P.J. Hasnip, S.J. Clark, M.C. Payne, First-principles simulation: ideas, illustrations and the CASTEP code. J. Phys. Condens. Mat. **14**, 2717 (2002)
50. J.P. Perdew, K. Burke, M. Ernzerhof, Generalized gradient approximation made simple. Phys. Rev. Lett. **77**, 3865–3868 (1996)
51. D. Vanderbilt, Soft self-consistent pseudopotentials in a generalized eigenvalue formalism. Phys. Rev. B **41**, 7892–7895 (1990)
52. V.G. Ruiz, W. Liu, E. Zojer, M. Scheffler, A. Tkatchenko, Density-functional theory with screened van der Waals interactions for the modeling of hybrid inorganic-organic systems. Phys. Rev. Lett. **108**, 146103 (2012)
53. J. Wellendorff, T.L. Silbaugh, D. Garcia-Pintos, J.K. Nørskov, T. Bligaard, F. Studt, C.T. Campbell, A benchmark database for adsorption bond energies to transition metal surfaces and comparison to selected DFT functionals. Surf. Sci. **640**, 36–44 (2015)
54. A. Tkatchenko, L. Romaner, O.T. Hofmann, E. Zojer, C. Ambrosch-Draxl, M. Scheffler, Van der Waals interactions between organic adsorbates and at organic/inorganic interfaces. MRS Bull. **35**, 435–442 (2011)
55. S.P. Liu, M. Zhao, W. Gao, Q. Jiang, Mechanistic insights into the unique role of copper in CO_2 electroreduction reactions. ChemSusChem **10**, 387–393 (2017)
56. N. Govind, M. Petersen, G. Fitzgerald, D. King-Smith, J. Andzelm, A generalized synchronous transit method for transition state location. Comput. Mater. Sci. **28**, 250–258 (2003)
57. D. Donadio, L.M. Ghiringhelli, L. Delle Site, Autocatalytic and cooperatively stabilized dissociation of water on a stepped platinum surface. J. Am. Chem. Soc. **134**, 19217–19222 (2012)
58. B.J. Hinch, L.H. Dubois, First-order corrections in modulated molecular beam desorption experiments. Chem. Phys. Lett. **171**, 131–135 (1990)
59. X.-K. Gu, W.-X. Li, First-principles study on the origin of the different selectivities for methanol steam reforming on Cu(111) and Pd(111). J. Phys. Chem. C **114**, 21539–21547 (2010)
60. J.B. Hansen, P.E. Højlund Nielsen, Methanol synthesis, in: handbook of heterogeneous catalysis, (Wiley-VCH Verlag GmbH & Co. KGaA, 2008)
61. A.A. Peterson, F. Abild-Pedersen, F. Studt, J. Rossmeisl, J.K. Norskov, How copper catalyzes the electroreduction of carbon dioxide into hydrocarbon fuels. Energy Environ. Sci. **3**, 1311–1315 (2010)